

# ASPECTS REGARDING THE DYNAMICS OF A BIOMEDICAL SYSTEM DESIGNED TO MEASURE INFERIOR LIMBS

CRISTIAN-GEORGE DRAGOMIRESCU<sup>1</sup>, IONEL BUJOREL PĂVĂLOIU<sup>2</sup>, RALUCA IOANA GUICĂ<sup>2</sup>

**Key words:** Biomedical system, Measurement accuracy in orthopedics, Sliding measuring system.

The paper describes an innovative system designed to allow pre-operative measurements to be performed on the bed of immobilized or difficult to move patients, waiting for the implantation of orthopedic surgical devices. For this purpose, particular attention is paid to measuring the lengths of different bone segments in the clinical examination phase, where the presence of a measurement system capable of providing information about the three-dimensional setting of certain bone margins is needed, accompanied by an easy handling by the medical staff. After the design presentation, we develop an analytical study by determining the differential equations of the movement, simulating the position of the probe with the ROBOTICS toolbox from the MATLAB environment, as well as the time variation of the considered parameters, depending on the non-linear differential equation systems and the values obtained with ROBOTICS.

## 1. INTRODUCTION

The paper describes an innovative system initiated in [1, 2], where several device models were presented, that could be applied in measuring the lengths in orthopedics. One of the proposed models was selected and analyzed in detail to highlight the importance of the chosen parameters and the evolution in time. The idea was started by the length difference of the people limbs, which is a condition characterized by a considerable discrepancy in their relative length. If this difference occurs in the lower limbs, it is known as the inferior limb inequality and is relatively common, with 65 % – 70 % of the population suffering from a form of this disorder [3]. Guichet shows in a study that a gap greater than 20 mm affects at least one in 1,000 people [4].

The length difference can be characterized as being real (structural), when it results from a disproportion of bone, or functional components, when it results from secondary deformations.

According to Reid and Smith, there are three categories of inequalities based on the magnitude of the discrepancy [5]: mild (difference < 30 mm); moderate (difference in the range from 30 to 60 mm); severe (difference > 60 mm). There is a disagreement in literature about the degree of inequality considered clinically significant, but there is a consensus that patients with a discrepancy greater than 20 mm are more likely to exhibit different symptoms [3].

Problems that may arise are various, including: back pain, compensatory scoliosis, high energy and oxygen consumption during walking, ankle contraction on the short leg side, osteoarthritis of the hip, fractures [6, 7]. In addition, biomechanical imbalances caused by inferior limb inequality appear to be one of the factors contributing to the production of injuries during running. Thus, Liu and colleagues reported that patients with inferior limb inequality developed various mechanisms in an attempt to compensate for this, including: increased leg flexion, shorter leg extension, shorter leg supination, and prone the longer leg [8].

The picture of the currently used methods for measuring the lengths of the inferior limbs, as shown by the analysis of the literature, is summarized as followed:

- **Clinical methods:** Using a *tape line* [9]; Placement of *wooden blocks* of different sizes under the shorter foot as alternative method [10]; *Inclinometer*; *The PALpation Meter* [11], which is a combination of an inclinometer and a compass, accompanied by a special ruler [5].
- **Preoperative measurement methods using imaging techniques:** They include both *Radiographic measurements of leg lengths, both in adults and children*: *Orthooronography*; *Scanography*; *Teleoroentgenography* [6], as well as *Computerized radiography*; *Low-dose digital radiography*; *Computer tomography* [12]; *Ultrasound* evaluation technique; *Nuclear Magnetic Resonance (NMR)*.
- **Intra-operative measurement methods:** Measurement between *fixed markers* around the hip joint; Using a *two-pin fixator-extractor* [7]; *Caliper compass*; *Templates* [2].
- **Use of lower limb analysis software:** *Conventional X-ray radiography* [6].

In order to obtain a better positioning of the bone segments, a measuring system is required to provide information about the three-dimensional positioning of certain known bone margins, thus creating the premise of obtaining the anatomical fracture reduction. The measuring device should have a low weight and size and an increased portability. This allows the medical staff to repeat the measurement conditions as fast as possible and to reduce the surgical procedure interval because of a user-friendly interface, avoiding the human errors that may occur in such situations.

Therefore, the aim of the paper is to increase the precision of measurement in orthopedics and to propose a metrological device that meets the requirements of the medical staff: the device should have low weight and size, to facilitate its use very fast, it must also be characterized by increased portability, allowing medical personnel to restore measurement conditions as quickly as possible.

## 2. PRESENTATION OF THE MODEL AND ANALYTICAL STUDY OF THE SYSTEM

The designed model [1] consists of a movable bed with a support frame and a four-degree distance measuring system

<sup>1</sup> University POLITEHNICA of Bucharest, Department of Mechanics, Bucharest, Romania, cristian\_dragomirescu@yahoo.com

<sup>2</sup> University POLITEHNICA of Bucharest, Department of Engineering in Foreign Languages, Bucharest, Romania

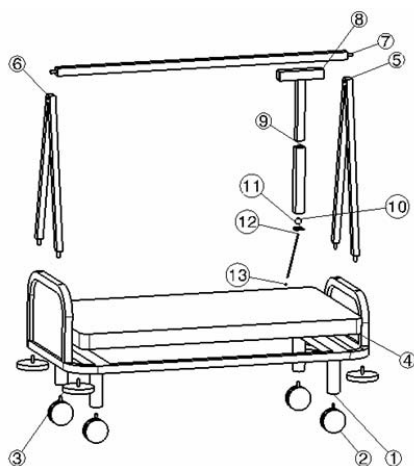


Fig. 1 – Bed frame designed model.

that can slide both along the longitudinal axis of the bed and in the vertical plane and can thus cover a spatial volume large enough to allow the necessary measurements.

As can be seen in Fig. 1, the model consists of a bed frame (1), four double wheels (2), which allow for increased maneuverability in narrow spaces; 4 simple side wheels (3) provide a easy sliding in case of impact with a rigid surface (salon / lift / etc); a mattress (4); support elements of the sliding rail (5) and (6), a profiled rail (7), allowing the entire measuring assembly to move along its length. The movable carriage (8) exhibits a linear Hall effect incremental transducer, which serves to monitor the position of the assembly along the rail axis.

Telescopic elements (9) allow varying the level of the measurement end, as required. Also, at its level there is a linear transducer, which has the role of sensing the variations of the vertical movement (in the  $z$ -axis direction) of the assembly and a spring-loaded springing system to cancel the weight effects of the assembly and keep it at a neutral level. The spherical joint (10) allows two degrees of freedom and is equipped with two incremental rotary transducers, with a resolution of 1000 impulses per rotation, mounted on two perpendicular axes (axes  $x$  and  $y$ ). The element (11) is a spherical hinge fastening cap and (12) is an enlarged stiffness measuring head provided with a ball probe (13) at its free end. The acquisition of the signals

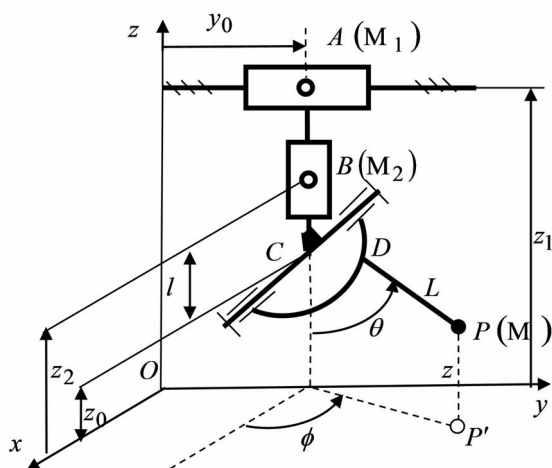


Fig. 2 – Analysis model.

from the three transducers can be performed using devices like the one from SynapseAndSilicon, programmed to display the angles and the displacements.

The design from Fig. 1 allows the realization of the analysis model shown in Fig. 2, which leads to the determination of the differential equations of the movement and implicitly to the development of the analytical study under the dynamic system, because the measurements are performed pre-, post- and during the operation. For the dynamic system in the examination position (the patient's bed is fixed), the coordinates of the point  $P$ , which represent the spherical probe, are written in relation to the entries from Fig. 2.

$$\begin{aligned} x &= L \sin \theta \cos \varphi \\ y &= y_0 + L \sin \theta \sin \varphi \\ z &= z_0 - L \cos \theta, \end{aligned} \quad (1)$$

which allows, by derivation, the determination of the components of the speed of the point corresponding to the coordinate axes:

$$\begin{aligned} \dot{x} &= L(\dot{\theta} \cos \theta \cos \varphi - \dot{\varphi} \sin \theta \sin \varphi) \\ \dot{y} &= \dot{y}_0 + L(\dot{\theta} \cos \theta \sin \varphi + \dot{\varphi} \sin \theta \cos \varphi) \\ \dot{z} &= \dot{z}_0 + L\dot{\theta} \sin \theta, \end{aligned} \quad (2)$$

and so calculating its speed module (2.3):

$$v^2 = \dot{x}^2 + \dot{y}^2 + \dot{z}^2. \quad (3)$$

It is thus possible to write the kinetic energy of the analyzed dynamic system:

$$E = \frac{1}{2} M_1 \dot{y}_0^2 + \frac{1}{2} M_2 \dot{z}_2^2 + \frac{1}{2} M v^2, \quad (4)$$

and the force-function:

$$U = -M_1 g z_1 - M_2 g z_2 - M g z_3 + C, \quad (5)$$

where  $M_1$  is the weight of the slide  $A$ ,  $M_2$  is the weight of the slide  $B$ ,  $M$  is the mass of the probe, which also includes the one of the rod  $DP$ ,  $C$  is a constant,  $z_1, z_2, z_3$  are the coordinates of the three masses in relation to the considered reference system,  $z_2 = z_0 + l$  represents the algebraic relationship between the elements in Fig. 2, and  $z_1 = K = \text{constant}$ .

With the obtained data we can determine the differential equations of the movement, for the analyzed system, with the Lagrange equations of the second order [13]:

$$\frac{d}{dt} \left( \frac{\partial E}{\partial \dot{q}_i} \right) - \frac{\partial E}{\partial q_i} = \frac{\partial U}{\partial q_i}, \quad i = 1, 2, 3, 4, \quad (6)$$

where  $E$  – represents the kinetic energy of the system,  $U$  – is his force function,  $q_1 = y_0, q_2 = z_0, q_3 = \theta, q_4 = \varphi$  – are the generalized coordinates, and  $\dot{q}_1 = \dot{y}_0, \dot{q}_2 = \dot{z}_0, \dot{q}_3 = \dot{\theta}, \dot{q}_4 = \dot{\varphi}$  – represent the generalized velocities.

It is found that the system considered is characterized by four independent parameters (four degrees of freedom), which leads after the calculations to the four differential equations of motion, respectively:

$$\begin{aligned}
& \ddot{y}_0(M_1 + M) + ML\ddot{\theta}\cos\theta\sin\varphi + ML\dot{\theta}\sin\theta\cos\varphi - \\
& - ML(\dot{\theta}^2 + \dot{\varphi}^2)\sin\theta\sin\varphi + 2ML\dot{\theta}\dot{\varphi}\cos\theta\cos\varphi = 0 \\
& \ddot{z}_0(M_2 + M) + ML\ddot{\theta}\sin\theta + ML\dot{\theta}^2\cos\theta = -g(M_2 + M) \quad (7) \\
& \ddot{y}_0\cos\theta\sin\varphi + \ddot{z}_0\sin\theta + L\ddot{\theta} - L\dot{\varphi}^2\sin\theta\cos\theta = -g\sin\theta \\
& \ddot{y}_0\sin\theta\cos\varphi + L\ddot{\varphi}\sin^2\theta + L\dot{\theta}\dot{\varphi}\sin 2\theta = 0,
\end{aligned}$$

which form a non-linear system that describes a movement example with four degrees of freedom. Starting from the general case described by the system (7), the following particular instances may also be studied:

- The *slide A* has reached the required measurement position and has no translational movement in the  $y$  direction ( $y_0 = \text{constant}$ ,  $\dot{y}_0 = 0$ ,  $\ddot{y}_0 = 0$ ). The system (7) becomes in this case a system of nonlinear differential equations describing a movement with three degrees of freedom.
- The *slides A and B* have reached the required position and no longer have translational movements in the  $y$  direction ( $y_0 = \text{constant}$ ,  $\dot{y}_0 = 0$ ,  $\ddot{y}_0 = 0$ ), respectively in the  $z$  direction ( $z_0 = \text{constant}$ ,  $\dot{z}_0 = 0$ ,  $\ddot{z}_0 = 0$ ).

The system (7) becomes in this case a system of non-linear differential equations describing a movement with two degrees of freedom.

### 3. SIMULATING THE POSITION OF THE TOUCH PROBE USING THE ROBOTICS TOOL SET

The scheme of this sliding system is shown in Fig. 3. This will lead to the finding of the spherical coordinates using Denavit-Hartenberg (D-H) parameters [14], then to simulate the system. MATLAB®, developed by Mathworks Inc, is a well known scientific and engineering development environment. A strong point of MATLAB® is the presence of toolboxes, libraries of topic-dedicated functions. The Robotics Toolbox for MATLAB® [15, 16], which offers a wide range of functions for simulation of mobile robots and articulated elements, has been used in this paper. The toolkit includes functions for manipulating and converting data types such as vectors, homogeneous transformations, angular representations that are required for the three-dimensional representation of the position and spatial orientation of the articulated systems, as well as for creating direct and inverse cinematics [15–17].

The model was designed to allow pre-operative measurements at the bed of immobilized or difficult to

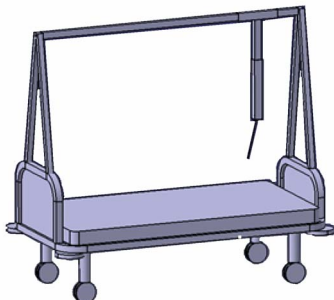


Fig. 3 – Sliding system on a bar attached above the patient's bed.

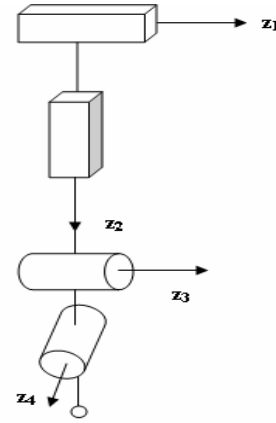


Fig. 4 – The kinematic scheme for the sliding system on a bar attached above the patient's bed.

move patients. The kinematic scheme of this sliding system (Fig. 4) is useful for determining the dimensions of the palpation sphere using D-H parameters, allowing a simulation with the Robotics tool set in the Matlab program to read the position of the two points, then calculate the distance between them.

The D-H parameters are combined into a 4 x 4 matrix, called homogenous transformation matrix  ${}^{i-1}T_i$ , which describes the orientation and position of a coordinate axis system  $i$ , in relation to the coordinate axis system,  $i-1$ . The homogenous transformation of D-H parameters is given in equation:

$${}^{i-1}T_i = \text{Rot}_z(\theta_i)\text{Trans}_z(d_i)\text{Trans}_x(a_i)\text{Rot}_x(\alpha_i) \quad (8)$$

The transformation is given by 2 rotations and two translations as follows:

A rotation along the  $z_{i-1}$  axis with an angle  $\theta_i$ .

A translation along  $z_{i-1}$  axis with a distance  $d_i$ .

A translation with a distance  $a_i$  along the  $x_i$  axis.

A rotation with an angle  $\alpha_i$ , along the  $x_i$  axis.

Taking into account the above equations and equation (8), it can be written that:

$$\begin{aligned}
{}^{i-1}T_i &= \begin{bmatrix} [A] & [B] & [C] & [D] \end{bmatrix}, \text{ with} \\
[A] &= \begin{bmatrix} \cos\theta_i \\ \sin\theta_i \\ 0 \\ 0 \end{bmatrix}; \quad [B] = \begin{bmatrix} -\sin\theta_i \cos\alpha_i \\ \cos\theta_i \cos\alpha_i \\ \sin\alpha_i \\ 0 \end{bmatrix}; \\
[C] &= \begin{bmatrix} \sin\theta_i \sin\alpha_i \\ -\cos\theta_i \sin\alpha_i \\ \cos\alpha_i \\ 0 \end{bmatrix}; \quad [D] = \begin{bmatrix} a_i \cos\theta_i \\ a_i \sin\theta_i \\ d_i \\ 1 \end{bmatrix}.
\end{aligned} \quad (9)$$

The values used for the D-H parameters are presented in Table 1.

Table 1

D-H (Denavit-Hartenberg) parameters for the sliding system on a bar attached above the patient's bed

The element	$\theta_i$	$d_i$	$a_i$	$\alpha_i$
1	90	$d_1$	0.4	90
2	0	$d_2$	0	90
3	$\theta_3$	0	0	90
4	$\theta_4$	0	0.3	0

Using the D-H parameters in Table 1 and the equation set (9), we determine the following transformation matrices:

$${}^0_1T = \begin{bmatrix} 0 & 0 & 1 & 0 \\ 1 & 0 & 0 & 0.4 \\ 0 & 1 & 0 & d_1 \\ 0 & 0 & 0 & 1 \end{bmatrix}, \quad (10)$$

$${}^1_2T = \begin{bmatrix} 1 & 0 & 0 & 0 \\ 0 & 0 & -1 & 0 \\ 0 & 1 & 0 & d_2 \\ 0 & 0 & 0 & 1 \end{bmatrix}, \quad (11)$$

$${}^2_3T = \begin{bmatrix} \cos\theta_3 & 0 & \sin\theta_3 & 0 \\ \sin\theta_3 & 0 & -\cos\theta_3 & 0 \\ 0 & 1 & 0 & 0 \\ 0 & 0 & 0 & 1 \end{bmatrix}, \quad (12)$$

$${}^3_4T = \begin{bmatrix} \cos\theta_4 & -\sin\theta_4 & 0 & 0.3\cos\theta_4 \\ \sin\theta_4 & \cos\theta_4 & 0 & 0.3\sin\theta_4 \\ 0 & 0 & 1 & 0 \\ 0 & 0 & 0 & 1 \end{bmatrix}, \quad (13)$$

$${}^2_4T = \begin{bmatrix} c_3c_4 & -c_3s_4 & s_3 & 0.3c_3c_4 \\ s_3c_4 & -s_3s_4 & -c_3 & 0.3s_3c_4 \\ s_4 & c_4 & 0 & 0.3s_4 \\ 0 & 0 & 0 & 1 \end{bmatrix}, \quad (14)$$

$${}^1_4T = {}^1_2T {}^2_4T = \begin{bmatrix} c_3c_4 & -c_3s_4 & s_3 & 0.3c_3c_4 \\ -s_4 & -c_4 & 0 & -0.3s_4 \\ s_3c_4 & -s_3s_4 & -c_3 & 0.3s_3c_4 + d_2 \\ 0 & 0 & 0 & 1 \end{bmatrix}, \quad (15)$$

$${}^0_4T = {}^0_1T {}^1_4T = \begin{bmatrix} s_3c_4 & -s_3s_4 & -c_3 & 0.3s_3c_4 + d_2 \\ c_3c_4 & -c_3s_4 & s_3 & 0.3c_3c_4 + 0.4 \\ -s_4 & -c_4 & 0 & -0.3s_4 + d_1 \\ 0 & 0 & 0 & 1 \end{bmatrix}. \quad (16)$$

Based on equation (16), the coordinates of the probe in relation to the base of the system are

$$p_x = 0.3s_3c_4 + d_2; p_y = 0.3c_3c_4 + 0.4; p_z = -0.3s_4 + d_1. \quad (17)$$

Once the D-H parameters are found, we can implement the sliding system attached to a bar over the patient's bed using the Robotics tool kit. The simulation uses a command window, as can be seen in Figs. 5 and 6. These command windows allow for varying the D-H parameters, displaying in real time the corresponding sliding system position, as can be seen in Figs. 7 and 8.

For the sliding assembly attached to a bar above the patient's bed, two random positions were taken as the initial and the final position, needed to simulate the movement and to find the two different locations of the palpable sphere in order to obtain the distance between them.

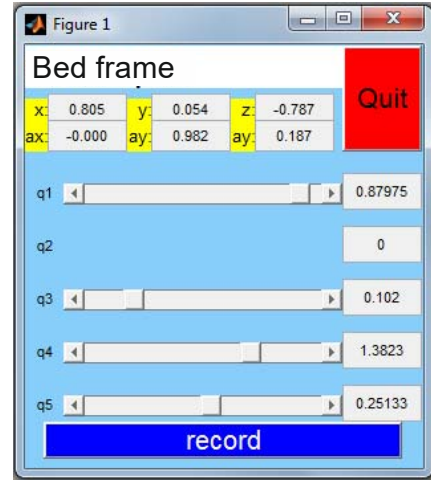


Fig. 5 – Coordinates of the sphere for the initial position.

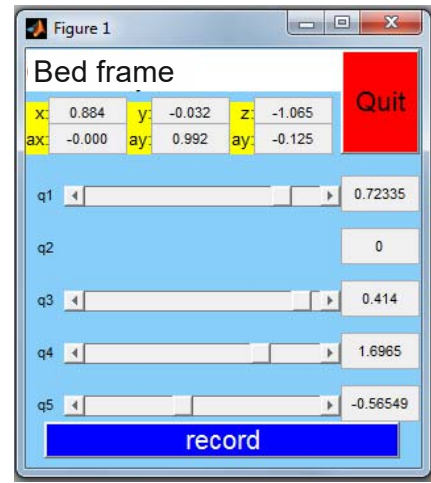


Fig. 6 – Coordinates of the sphere for the final position.

So for the initial position in Fig. 5 of the articulated arm, the coordinates of the sphere are:  $x_1 = 0.805$ ,  $y_1 = 0.054$ ,  $z_1 = -0.787$  and for the final position in Fig. 6, after the D-H parameters have been changed, sphere coordinates are:  $x_2 = 0.884$ ,  $y_2 = -0.032$ ,  $z_2 = -1.065$

Thus, for these two particular cases, the distance  $d$  between the two points is  $d = 301$  mm.

In Figs. 7 and 8 there are represented the initial and the final positions of the sliding system.

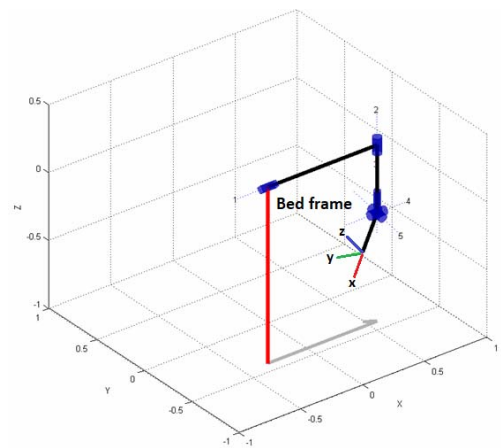


Fig. 7 – The initial position of the sliding system on a bar above the patient's bed.

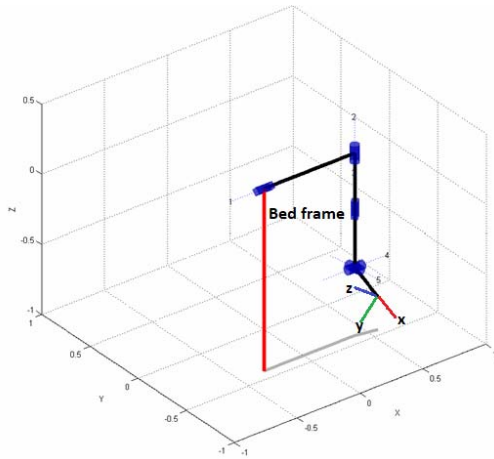


Fig. 8 – The final position of the sliding system on a bar above the patient's bed.

Using the differential equations of movement and the numerical values determined in the particular cases presented in the previous chapter, the graphical representations of time variations of the parameters are obtained.

The case of the nonlinear system with four degrees of freedom (7), as well as the particular cases derived from the successive loss of the possibilities of movement due to the medical intervention stage are analyzed

The following representations are found:

- for the nonlinear differential equation system with four degrees of freedom

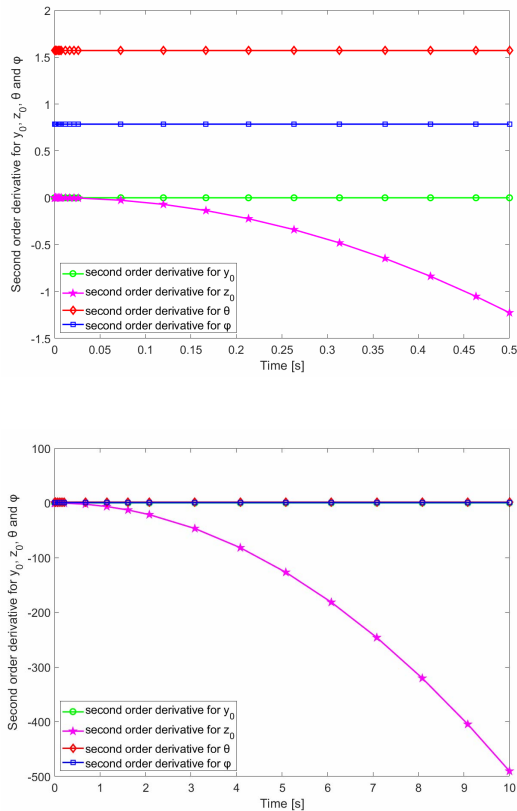


Fig. 9 – System with four degrees of freedom

Qualitative analysis reveals the same aspect of graphical representations as for  $t = 10$  s and for  $t = 1000$  s.

- for the nonlinear differential equation system with three degrees of freedom ( $y_0 = \text{constant}$ )

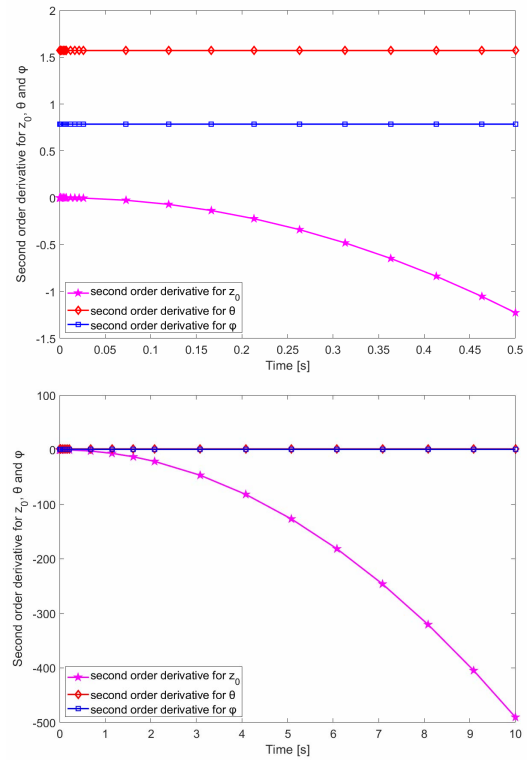


Fig. 10 – System with three degrees of freedom

Qualitative analysis reveals the same aspect of graphical representations as for  $t = 5$  s and for  $t = 1000$  s.

- for the nonlinear differential equation system with two degrees of freedom ( $y_0, z_0 = \text{constant}$ )

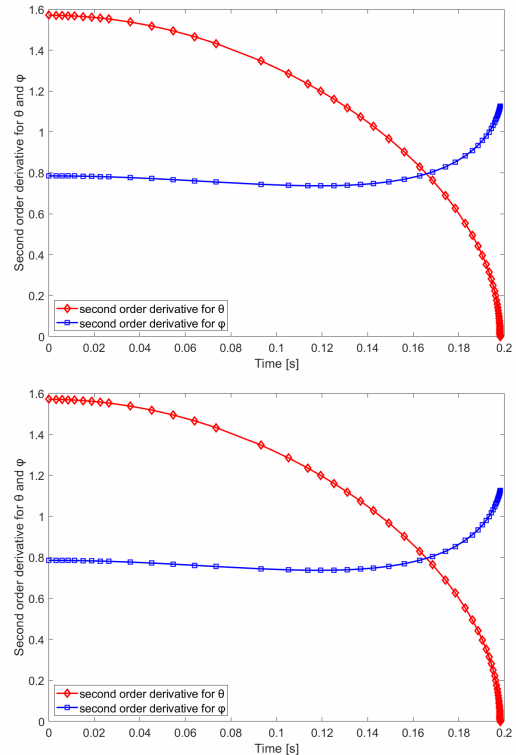


Fig. 11 – System with two degrees of freedom

Qualitative analysis reveals the same aspect of graphical representations as for  $t = 0.5$  s and for  $t = 1000$  s.

Several such variations in time of the analyzed elements were made and only two representations were recorded in each case, which revealed the evolution of the analyzed elements and showed that the qualitative aspect is preserved over time and correspond to the types of movements analyzed. This way the position is known at each moment and the results from the Robotics analysis are validated.

#### 4. CONCLUSIONS

The paper continues the research on the increase of measurement accuracy in orthopedics [1] by proposing an innovative system designed to allow preoperative measurements to be performed on the bed of difficult to move patients for the implantation of orthopedic surgical devices.

An analytical study was carried out, which we have not found in other bibliographic references and which theoretically substantiates the movements that take place during all phases of the operation (pre-, post-, during). It checks and confirms the evolution in time of the laws of motion, which preserves its qualitative character over the time frame considered.

In this respect, the dynamics of a biomedical system designed to measure the lower limbs, using non-linear differential equations of movement, is analyzed through a MATLAB program.

The proposed analysis model takes into account the particular clinical aspects from specific cases in medical practice, highlighting the time variation of active elements during the intervention period on the patient.

Starting from the data obtained with the ROBOTICS tools in the MATLAB environment, there are exemplified the graphs corresponding to the system with four degrees of freedom considered respectively as those with three and two degrees of freedom, which represent the original system's particularity for situations in which certain parameters become constant. The qualitative analysis of the time variation of the considered parameters allows insight into the displacement of the constructive elements from the dynamic system at certain time instants, indicating the type of movement and its characteristics. The practitioners gain thus information about the system dynamics, contributing to improved medical performance and efficient use of the device.

Received on May 23, 2019

#### REFERENCES

1. R. I. Guică, *Cercetări privind creșterea preciziei de măsurare în ortopedie- Teză de doctorat*, Universitatea POLITEHNICA din București, 2012
2. R. I. Guică, Cristian Dragomirescu, L. E. Trifan; C. A. Micu, *A New Approach Of A Length Measuring System In Orthopedics Using A Laser Probe*, Proceedings in Manufacturing Systems, 7, 4, pp. 269–274 (2012).
3. B. S. Ball, *A technique for comparison of leg lengths during total hip replacement*. Am J Orthop., 25, 1, 61–62 (1996).
4. J.M. Guichet, J.M. Spivak, P. Trouilloud, P.M. Grammont, *Lower limb-length discrepancy. An epidemiologic study*. Clin. Orthop., 272, pp. 235–241, (1991).
5. D. C. Reid, B. Smith, *Leg length inequality: a review of etiology and management*, PhysioCan, 36, pp. 177–182 (1984).
6. S. Sabharwal, C. Zhao, J. Mckeon, T. Melaghari, M. Blacksin, C. Wenekor, *Reliability analysis for radiographic measurement of limb length discrepancy: full-length standing anteroposterior radiograph versus scanogram*. J Pediatric Orthop., 27, pp. 46–50 (2007).
7. I. Takigami, M. Itokazu, Y. Itoh, K. Matsumoto, T. Yamamoto, K. Shimizu, *Limb-Length Measurement in Total Hip Arthroplasty Using a Calipers Dual Pin Retractor*; Bulletin of the NYU Hospital for Joint Diseases, 66, 2, pp. 107–110(2008).
8. X.C. Liu, G. Fabry, G. Molenaers, J. Lammens, P. Moens, *Kinematic and kinetic asymmetry in patients with leg-length discrepancy*. J Pediatr Orthop., 18, pp. 187–189(1998).
9. P. Beattie, K. Isaacson, D.L. Riddle, J.M. Rothstein, *Validity of derived measurements of leg-length differences obtained by use of a tape measure*. Phys Ther, 70, 3, pp. 150–157 (1990).
- 10., H.I.H. Lampe; B.A. Swierstra, A.F.M. Diepstraten, *Measurement of limb length inequality. Comparison of clinical methods with orthoradiography in 190 children*, Acta orthop Scand, 67, 3, pp. 242–244 (1996).
11. M. R. Petrone, J. Guinn, A. Reddin, T.G. Sutlive, T.W. Flynn, M.P. Garber, *The Accuracy of the Palpation Meter (PALM) for Measuring Pelvic Crest Height Difference and Leg Length Discrepancy*, Journal of Orthopaedic & Sports Physical Therapy, 33, pp. 319–325 (2003).
12. E. Segev, Y. Hemo, S. Wientroub, D. Ovadia, M. Fishkin, D.M. Steinberg, S. Hayek, *Intra- and interobserver reliability analysis of digital radiographic measurements for pediatric orthopedic parameters using a novel PACS integrated computer software program*, J Child Orthop, 4, pp. 331–341 (2010).
13. R. Voinea, E. Deciu, C. Dragomirescu, *Technische Mechanik*, Editura ALMA Craiova, 2009
14. L. Vlădăreanu, A. Curaj, R.I. Munteanu, *Complex Walking Robot Kinematics Analysis and PLC Multi-Tasking Control*, Rev. Roum. Sci. Techn. – Électrotechn. et Énerg., 57, 1, pp. 90–99 (2012).
15. P. Corke, *Robotics, Vision and Control, Fundamental Algorithms in MATLAB®*, Ed. Springer, Berlin 2011.
16. P. Corke, *Robotics Toolbox for Matlab*, available at <https://petercorke.com/wordpress/toolboxes/robotics-toolbox>.
17. A. Nagchadhuri, *Experience with Introducing Robotics Toolbox for MATLAB in a Senior Level Undergraduate Course*, University of Maryland Eastern Shore Department of Engineering and Aviation Science; Proceedings of IMECE'09 ASME International Mechanical Engineering Congress and Exposition November 13–19, Lake Buena Vista, Florida, USA (2009).